Chin. J. Astron. Astrophys. Vol. 6 (2006), No. 1, 52–60
(*http://www.chjaa.org*)

Chinese Journal of
Astronomy and
Astrophysics

The Relationship between the Rise Width and the Full Width of γ-ray Burst Pulses and Its Implications *

Rui-Jing Lu[1,2,3], Yi-Ping Qin[1,2] and Ting-Feng Yi[2]

[1] National Astronomical Observatories/Yunnan Observatory, Chinese Academy of Sciences, Kunming 650011; *luruijing@126.com; ypqin@ynao.ac.cn*
[2] Department of Physics, Guangxi University, Nanning, Guangxi 530004
[3] Graduate University of Chinese Academy of Sciences, Beijing 100049

Received 2005 June 21; accepted 2005 September 7

Abstract We investigate the relationship between the rise width and the full width of gamma-ray burst pulses. Theoretical analysis shows that either width is proportional to $\Gamma^{-2}\Delta\tau_{\theta,\mathrm{FWHM}}\frac{R_c}{c}$ (Γ the Lorentz factor of the bulk motion, $\Delta\tau_{\theta,\mathrm{FWHM}}$ a local pulse's width, R_c the radius of fireballs and c the velocity of light). We study the relationship for four samples of observed pulses. We find: (1) merely the curvature effect could reproduce the relationship between the rise and full widths with the same slope as derived from the model of Qin et al.; (2) gamma-ray burst pulses, selected from both the short and long GRBs, follow the same sequence in the rise width vs. full width diagram, with the shorter pulses at one end; (3) all GRBs may intrinsically result from local Gaussian pulses. These features place constraints on the physical mechanism(s) for producing long and short GRBs.

Key words: gamma rays: bursts – gamma rays: theory – methods: data analysis

1 INTRODUCTION

Although the mechanism underlying gamma-ray bursts is still unclear, it is generally accepted that the large energies and the short timescales involved require the gamma-rays to be produced in a sort of fireball in relativistic expansion (see, e.g., Goodman 1986; paczynski 1986). An individual shock episode gives rise to a pulse in the gamma-ray light curve, and superposition of many such pulses creates the observed diversity and complexity of the light curves (Fishman et al. 1994). Therefore, the temporal characteristics of these pulses hold the key to the understanding of the prompt radiation of gamma-ray bursts. It is generally believed that some well-separated individual pulses represent the fundamental constituents of the GRB time profile (light curve) and the pulses are asymmetrical with a fast rise and an exponential decay (FRED).

What does result in the observed light curves? According to Ryde & Petrosian (2002), the simplest scenario accounting for the observed GRB pulses is to assume an impulsive heating of the leptons and a subsequent cooling and emission. In this scenario, the rising phase of the pulse, which is referred to as the dynamic time, arises from the energizing of the shell, while the decay phase reflects the cooling and its timescale. However, in general, the cooling time for the relevant

* Supported by the National Natural Science Foundation of China.

parameters is too short to explain the pulse durations and the resulting cooling spectra are not consistent with observation (Ghisellini et al. 2000). As shown by Ryde & Petrosian (2002), this problem could be solved when the curvature effect of the expanding fireball surface is taken into account.

The morphological diversity of gamma-ray light curves could be interpreted within the standard fireball model (Rees & Mészáros 1992), and the observed FRED structure was found to be interpretable by the curvature effect as the observed plasma moves relativistically towards us and appears to be locally isotropic (e.g., Fenimore et al. 1996; Ryde & Petrosian 2002; Kocevski et al. 2003, hereafter Paper I). Several investigations on modeling pulse profiles have been made (e.g., Norris et al. 1996; Lee et al. 2000a, 2000b; Ryde & Svensson 2000; Ryde & Petrosian 2002; Borgonovo & Ryde 2001; Paper I), they derived several flexible functions to describe the profiles of individual pulses based on empirical or semi-empirical relations. For example, as derived in detail in Paper I, an FRED pulse can be well described by equations (22) or (28). Using this model, they found that there is a linear relationship between the full width at half-maximum (FWHM) and the rise width of the burst pulse detected by the BATSE instrument (see fig. 10 in paper I), and the same result can be found in the gamma-ray burst pulses detected by the anti-coincidence shield of the spectrometer (SPI) of INTEGRAL (see fig. 5a in Ryde et al. 2003).

Qin (2002) derived in detail the flux function based on the model of highly symmetric expanding fireball, where the Doppler effect of the expanding fireball surface is taken to be the key factor, and then with this formula Qin (2003) studied how emission and absorption lines are affected by the effect. Recently, Qin et al. (2004) presented the formula in terms of count rates. This model led to the unveiling of certain relations, a power law relationship between the observed pulse width and energy (Qin et al. 2005a), an anti-correlation between the power law index and the local pulse width (Jia et al. 2005), and correlations between spectral lags and such physical parameters as the Lorentz factor and the fireball radius (Lu et al. 2005a). At the same time, some characteristics have been found, such as a reverse S-feature curve in the decay phase (Qin et al. 2005b) and an inflexion from concavity to convexity in the rising phase (Lu et al. 2005b) of the light curve determined by equation (21) of Paper II. These findings, taken together, suggest a potential relationship between the rise width and the full width of the observed pulse, which motivates us to investigate the relationship found by Kocevski et al. based on Qin's model and to explore its implications in terms of the fireball model.

Although the origins of short GRBs and long GRBs are not yet clear, it is generally suggested that short GRBs are likely to be produced by the merger of compact objects while the long GRBs, by the core collapse of massive stars (see Zhang & Mészáros 2004; Piran 2005). The fact that the long and short GRBs have many similar properties including luminosity, $\langle V/V_{\max}\rangle$, the angular distribution, the energy dependence of the duration, the hard-to-soft spectral evolution, even the pulse profile (e.g., Schmidt 2001; Ramirez-Ruiz & Fenimore 2000; Lamb et al. 2002; Ghirlanda et al. 2004; Cui et al. 2005) indicates that the long and short GRBs may have the same emission mechanism but possibly different progenitors. Motivated by this, we also investigate the temporal structure of narrow pulses with durations shorter than 1 s (FWHM) from both short and long GRBs.

This paper is organized as follows. In Section 2, we investigate the temporal characteristics of the GRB light curves based on Qin's model. In Section 3 we examine the relationship between the rise width and the full width of observational pulses and explore its possible implication in terms of the fireball model. A discussion and conclusions will be presented in the last section.

2 THE THEORETICAL ANALYSIS

As derived in detail in paper II, the expected count rate of the fireball within frequency interval $[\nu_1, \nu_2]$ can be calculated with

$$C(\tau) = \frac{2\pi R_{\rm c}^3 \int_{\widetilde{\tau}_{\theta,\min}}^{\widetilde{\tau}_{\theta,\max}} \widetilde{I}(\tau_\theta)(1+\beta\tau_\theta)^2(1-\tau+\tau_\theta)d\tau_\theta \int_{\nu_1}^{\nu_2} \frac{g_{0,\nu}(\nu_{0,\theta})}{\nu}d\nu}{hcD^2\Gamma^3(1-\beta)^2(1+k\tau)^2}. \quad (1)$$

In above formula, τ_θ is a dimensionless relative local time defined by $\tau_\theta \equiv c(t_\theta - t_{\rm c})/R_{\rm c}$, where t_θ is the emission time in the observer frame, called local time, of photons emitted from the concerned differential surface ds_θ of the fireball (θ is the angle to the line of sight), t_c is a constant which could be assigned to any values of t_θ, and R_c is the radius of the fireball measured at $t_\theta = t_c$; the variable τ is a dimensionless relative time defined by $\tau \equiv [c(t - t_c) - D + R_c]/R_c$, where D is the distance of the fireball to the observer, and t is the observation time; $\widetilde{I}(\tau_\theta)$ represents the development of the intensity magnitude in the observer frame, called a local pulse function; $g_{0,\nu}(\nu_{0,\theta})$ describes the rest frame radiation mechanism, and $k \equiv \beta/(1-\beta)$. The integration limits $\widetilde{\tau}_{\theta,\rm min}$ and $\widetilde{\tau}_{\theta,\rm max}$ are determined by $\widetilde{\tau}_{\theta,\rm min} = \max\{\tau_{\theta,\rm min}, (\tau - 1 + \cos\theta_{\rm max})/(1-\beta\cos\theta_{\rm max})\}$ and $\widetilde{\tau}_{\theta,\rm max} = \min\{\tau_{\theta,\rm max}, (\tau - 1 + \cos\theta_{\rm min})/(1-\beta\cos\theta_{\rm min})\}$, where $\tau_{\theta,\rm min}$ and $\tau_{\theta,\rm max}$ are the lower and upper limits of τ_θ confining $\widetilde{I}(\tau_\theta)$, $\theta_{\rm min}$ and $\theta_{\rm max}$ are determined by the concerned area of the fireball surface, and then the radiation is observable within the range of $(1-\cos\theta_{\rm min}) + (1-\beta\cos\theta_{\rm min})\tau_{\theta,\rm min} \le \tau \le (1-\cos\theta_{\rm max}) + (1-\beta\cos\theta_{\rm max})\tau_{\theta,\rm max}$.

Equation (1) suggests that, the light curves of the sources depend mainly on Γ, $\widetilde{I}(\tau_\theta)$ and $g_{0,\nu}(\nu_{0,\theta})$. Observation suggests that the common radiation form of GRBs is the so-called Band spectrum function (Band et al. 1993) which was frequently, and rather successfully, employed to fit the spectra of the sources (see, e.g., Schaefer et al. 1994; Ford et al. 1995; Preece et al. 1998, 2000), therefore we take in this paper the Band function as the rest frame radiation form. Furthermore the rise width and the full width of light curves depend on the two factors, Γ and $\widetilde{I}(\tau_\theta)$.

In this paper, we denote by τ_r and $\tau_{\rm FWHM}$ the rise width and the full width of the light curve corresponding to variable τ, and by t_r and $t_{\rm FWHM}$, the same corresponding to variable t. In the same way, we denote by $\Delta\tau_{\theta,\rm FWHM}$ the FWHM of a local pulse corresponding to variable τ_θ, and by $\Delta t_{\theta,\rm FWHM}$, that corresponding to variable t_θ.

For the sake of simplicity, we first examine a local pulse with a power law rise and a power law decay:

$$\widetilde{I}(\tau_\theta) = I_0 \begin{cases} \left(\frac{\tau_\theta - \tau_{\theta,\rm min}}{\tau_{\theta,0} - \tau_{\theta,\rm min}}\right)^\mu & (\tau_{\theta,\rm min} \le \tau_\theta \le \tau_{\theta,0}) \\ \left(1 - \frac{\tau_\theta - \tau_{\theta,0}}{\tau_{\theta,\rm max} - \tau_{\theta,0}}\right)^\mu & (\tau_{\theta,0} < \tau_\theta \le \tau_{\theta,\rm max}) \end{cases} \tag{2}$$

with $\tau_{\theta,0}$ and μ constants. The FWHM of this local pulse is $\Delta\tau_{\theta,\rm FWHM} = (1 - 2^{(-1/\mu)})(\tau_{\theta,\rm max} - \tau_{\theta,\rm min})$. The relationships between τ_r, $\tau_{\rm FWHM}$ and Γ, and that between τ_r, $\tau_{\rm FWHM}$ and $\Delta\tau_{\theta,\rm FWHM}$ for the light curves determined by Equation (1) are plotted in Figure 1. The correlation between the τ_r and the $\tau_{\rm FWHM}$ of the light curves is presented in Figure 2.

Figure 1 shows that τ_r and $\tau_{\rm FWHM}$ decrease with the Lorentz factor following $\tau_r \propto \Gamma^{-2}$ and $\tau_{\rm FWHM} \propto \Gamma^{-2}$, and increase with $\Delta\tau_{\theta,\rm FWHM}$ following $\tau_r \propto \Delta\tau_{\theta,\rm FWHM}$ for every value of $\Delta\tau_{\theta,\rm FWHM}$, and $\tau_{\rm FWHM} \propto \Delta\tau_{\theta,\rm FWHM}$ when $\Delta\tau_{\theta,\rm FWHM} \ge 1$. Thus we obtain

$$\tau_r = k_1\Gamma^{-2}\Delta\tau_{\theta,\rm FWHM} = k_1 p, \tag{3}$$

$$\tau_{\rm FWHM} = k\Gamma^{-2}\Delta\tau_{\theta,\rm FWHM} = kp \qquad (\Delta\tau_{\theta,\rm FWHM} \ge 1), \tag{4}$$

where $p = \Gamma^{-2}\Delta\tau_{\theta,\rm FWHM}$, $k_1 = 0.597 \pm 0.006$ and $k = 1.335 \pm 0.036$ for this local pulse. It is found that each of the two quantities, τ_r and $\tau_{\rm FWHM}$, is proportional to p, but independent of Γ or $\tau_{\theta,\rm FWHM}$.

Considering the relation between τ and t, we obtain from Equations (3) and (4),

$$t_r = k_1 p \frac{R_c}{c}, \tag{5}$$

and

$$t_{\rm FWHM} = kp\frac{R_c}{c} \qquad (\Delta\tau_{\theta,\rm FWHM} \ge 1). \tag{6}$$

We find from the left panel of Figure 2 that τ_r increases linearly with $\tau_{\rm FWHM}$ when we take $\Delta\tau_{\theta,\rm FWHM}$ = constant and Γ = variable. So we perform a linear least square fit to the two quantities, and have $\log(\tau_r) = A + B\log(\tau_{\rm FWHM})$ for a certain value of $\Delta\tau_{\theta,\rm FWHM}$. The slope B almost the same for different values of $\Delta\tau_{\theta,\rm FWHM}$, whereas the intercept "A" changes from –1.981 to –0.526 as $\Delta\tau_{\theta,\rm FWHM}$ changes from 0.001 to 0.1. Also, there is an upper limit value of A$\simeq -0.40$ when $\Delta\tau_{\theta,\rm FWHM} \ge 1$, thus a dead line can be found when $\Delta\tau_{\theta,\rm FWHM} \ge 1$, i.e., $\log(\tau_r) = -0.404 + 1.00 \times$

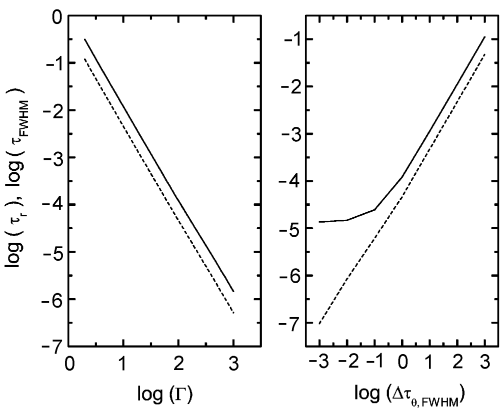

Fig. 1 Relationships between τ_r, $\tau_{\rm FWHM}$ and Γ (left panel) and those between τ_r, $\tau_{\rm FWHM}$ and $\Delta\tau_{\theta,\rm FWHM}$ (right panel) for the light curves determined by Eq. (1), where a Band function rest frame radiation form with $\alpha_0 = -1$ and $\beta_0 = -2.25$, within the frequency range of $100 \le \nu/\nu_{0,p} \le 300$, is adopted, and we take $2\pi R_c^3 I_0/hcD^2 = 1$, $\mu = 2$, $\tau_{\theta,\min} = 0$, $\theta_{\min} = 0$, $\theta_{\max} = \pi/2$, $\Delta\tau_{\theta,\rm FWHM}$=1 in the left panel, and Γ=100 in the right panel. The solid and the dash line represent respectively $\tau_{\rm FWHM}$ and τ_r in both panels.

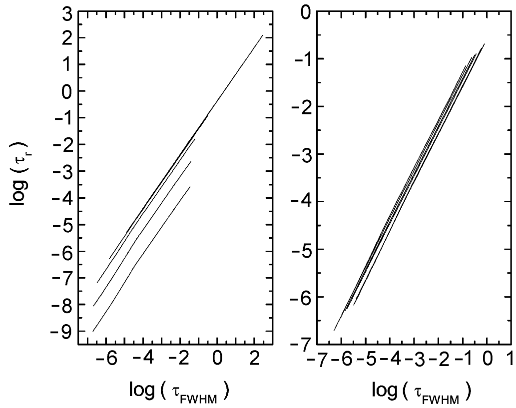

Fig. 2 Relationships between τ_r and $\tau_{\rm FWHM}$ for the light curves determined by Eq. (1). Left panel: We take Γ=2 to 1000 for different values of $\Delta\tau_{\theta,\rm FWHM}$. The solid lines from the bottom to the top represent $\Delta\tau_{\theta,\rm FWHM}$=0.001, 0.01, 0.1, 1, 10, 100, and 1000, respectively (note: when $\Delta\tau_{\theta,\rm FWHM} \ge 1$, their corresponding lines overlap each other). Right panel: the dead lines of the six local pulse forms: the solid lines from the bottom to the top represent local exponential rise and exponential decay pulse, local Gaussian pulse, local power law pulse μ=3, 2, 1 of Eq. (2) and local rectangle pulse, respectively. Other parameters are the same as those adopted in Fig. 1.

log($\tau_{\rm FWHM}$) (for all the fittings, the correlation coefficient $R > 0.999$ and the number of data points $N = 27$).

According to equations (6) and (7) of Paper II, one could find that the photons that observer receives at different observation times τ were emitted from different surface of the fireball when $\Delta\tau_{\theta,\rm FWHM} < 1$, so that the profiles of the light curves determined by Equation (1) are affected by $\Delta\tau_{\theta,\rm FWHM}$. Whereas when $\Delta\tau_{\theta,\rm FWHM} \ge 1$, the photons reaching the observer at different times τ come from the same whole surface of the fireball. In this case the profiles of the light curves do not change with $\Delta\tau_{\theta,\rm FWHM}$. This analysis is supported by the fact that τ_r is sensitive to the $\Delta\tau_{\theta,\rm FWHM}$, while $\tau_{\rm FWHM}$ is not significantly affected by $\Delta\tau_{\theta,\rm FWHM}$. When $\Delta\tau_{\theta,\rm FWHM} < 1$, $\tau_{\rm FWHM}$ slightly decreases with $\Delta\tau_{\theta,\rm FWHM}$, and in fact when $\Delta\tau_{\theta,\rm FWHM} \to 0$, the local pulse becomes a δ function, and $\tau_{\rm FWHM}$ would be determined by equation (44) in Paper II. However, when $\Delta\tau_{\theta,\rm FWHM} \ge 1$, each of the two quantities, τ_r and $\tau_{\rm FWHM}$, linearly increases with $\Delta\tau_{\theta,\rm FWHM}$ with the same slope (see the right panel of Fig. 1), which naturally explains why one could find a dead line in the τ_r–$\tau_{\rm FWHM}$ panel when $\Delta\tau_{\theta,\rm FWHM} \ge 1$.

Changing the frequency interval from $100 \le \nu/\nu_{0,p} \le 300$ to $25 \le \nu/\nu_{0,p} \le 50$, or to other frequency interval, and repeating the same work as above, we find that the results do not change significantly: the dead line is not sensitive to the frequency interval used.

We studied other forms of local pulses, such as $\mu = 1, 3$ of Equation (2), an exponential rise and exponential decay pulse, a Gaussian pulse, and a rectangle pulse, and so on, and found that Equations (3)–(6) hold for all the local pulses we investigated, and there are different values of k_1 and k for different local pulse forms (see Table 1). For every form of local pulse, a dead line could be found when $\Delta\tau_{\theta,\rm FWHM} \ge 1$. The dead lines of the six local pulses, $\log(\tau_r) = (-0.563 \pm 0.005) + (1.015 \pm 0.002)\log(\tau_{\rm FWHM})$ for the local exponential pulse, $\log(\tau_r) = (-0.520 \pm 0.009) + (1.027 \pm 0.003)\log(\tau_{\rm FWHM})$ for the local Gaussian pulse, $\log(\tau_r) = (-0.450 \pm 0.003) + (1.005 \pm 0.001)\log(\tau_{\rm FWHM})$ for $\mu = 3$ in Equation (2), $\log(\tau_r) = (-0.404 \pm 0.006) + (1.007 \pm 0.001)\log(\tau_{\rm FWHM})$ for $\mu = 2$ in Equation (2), $\log(\tau_r) = (-0.318 \pm 0.005) + (1.011 \pm 0.001)\log(\tau_{\rm FWHM})$ for $\mu = 1$ in Equation (2), and $\log(\tau_r) = (-0.221 \pm 0.011) + (1.027 \pm 0.003)\log(\tau_{\rm FWHM})$ for the local rectangle pulse, are displayed in the right panel of Figure 2.

Table 1 Coefficients for Equations (3) and (4)

Local pulse forms	k_1	k
$\mu = 1$ of Equation(2)	0.412 ± 0.003	0.827 ± 0.022
$\mu = 2$ of Equation(2)	0.597 ± 0.006	1.335 ± 0.036
$\mu = 3$ of Equation(2)	0.717 ± 0.009	1.718 ± 0.041
An exponential rise and decay pulse	0.306 ± 0.001	2.006 ± 0.122
A Gaussian pulse	0.650 ± 0.007	2.782 ± 0.149
A rectangle pulse	0.149 ± 0.001	0.318 ± 0.013

Our study showed that, for all forms of local pulse, the dead lines in the τ_r–$\tau_{\rm FWHM}$ panel always have slopes 1.0, but the intercepts are different. The intercept could therefore serve as an indicator of the local pulse form. We also note that the dead line of the local rectangle form is the upper limit of all local pulse forms (i.e., the intercept of the dead line for any local pulse form would never exceed –0.20), which might be a criterion to check if the temporal behaviors of gamma-ray burst pulses do result from the contributions from the Doppler effect.

3 RELATIONSHIP BETWEEN THE OBSERVED RISE TIME AND WIDTH OF PULSES

Kocevski et al. (2003) found that there is a linear correlation between the rise width and the full width of gamma-ray burst pulses observed by the BATSE instrument on board the CGRO (Compton Gamma Ray Observatory) spacecraft. For the sake of convenience of comparison with the results obtained theoretically above, unlike Kocevski et al., we here investigate the temporal structures of the light curves of the 2nd and 3rd channels based on their sample, respectively, which we call sample 1. As they pointed out that a power-law rise model can better describe the majority of the FRED pulses, so we measure t_r and $t_{\rm FWHM}$ of the pulses by fitting with equation (22) of their paper. The results are presented in Figure 3.

Figure 3 shows that t_r increases linearly with $t_{\rm FWHM}$ of the observed pulses. We perform a linear least square fit to the two quantities and obtain, at the 1σ confidence level, for the 2nd channel, $\log(t_r) = (-0.531 \pm 0.022) + (1.045 \pm 0.029)\log(t_{\rm FWHM})$ with a linear correlation coefficient of 0.973 and a chance probability of $p < 10^{-4}$, and for the 3rd channel, $\log(t_r) = (-0.492 \pm 0.029) + (1.031 \pm 0.024)\log(t_{\rm FWHM})$ with a linear correlation coefficient of 0.980 and a chance probability of $p < 10^{-4}$. The results show that the two sequences in the t_r–$t_{\rm FWHM}$ panel have almost the same intercepts and slopes within their errors. Intriguingly, one can find that the slope is equal to the one obtained theoretically above, which indicates that the observed results are well consistent with those predicted by Qin's model.

We thus may come to the following conclusions: (1) merely the curvature effect can produce the relationship in the $t_r - t_{\rm FWHM}$ panel which is independent of any frequency interval; (2) the gamma-ray burst pulses most probably arise from local Gaussian form because the sequences in the $t_r - t_{\rm FWHM}$ panel is closed to the dead line of local Gaussian form. Note that the differences between the two panels, τ_r-$\tau_{\rm FWHM}$ and t_r–$t_{\rm FWHM}$, do not affect the comparison (see Sect. 4).

To further demonstrate these conclusions, we choose another sample, called sample 2, based on gamma-ray burst pulses detected by the instrument HETE-2. Like Kocevski (2003), we select pulses from the HETE-2 burst home page (http://space.mit.edu/HETE/Bursts/) with the simple criterion that pulses show clean, well distinguished FRED-like form: this resulted 12 pulses in our sample 2. We measure t_r and $t_{\rm FWHM}$ of these pulses with the same methods as above, and the results are presented in Figure 4. We perform a linear least square fit to the two quantities with the same methods adopted in Figure 3, and obtain, for the band B, $\log(t_r) = (-0.494 \pm 0.065) + (1.012 \pm 0.087) \log(t_{\rm FWHM})$ with a linear correlation coefficient of 0.960 and a chance probability of $p < 10^{-4}$ and for for the band C, $\log(t_r) = (-0.504 \pm 0.059) + (1.088 \pm 0.078) \log(t_{\rm FWHM})$ with a linear correlation coefficient of 0.976 and a chance probability of $p < 10^{-4}$. The results are entirely consistent with those obtained from Figure 3, which further testify that the sequences in the t_r–$t_{\rm FWHM}$ plane is independent of any frequency interval.

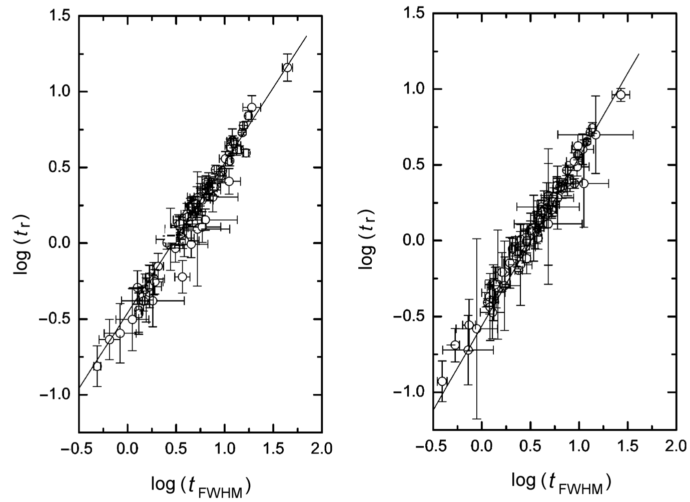

Fig. 3 Relationships between t_r and $t_{\rm FWHM}$ for the observed pulses based on sample 1. The left and the right panel present the pulses of the 2nd channel and the 3rd channel, respectively. The two solid lines are the fit lines of their data.

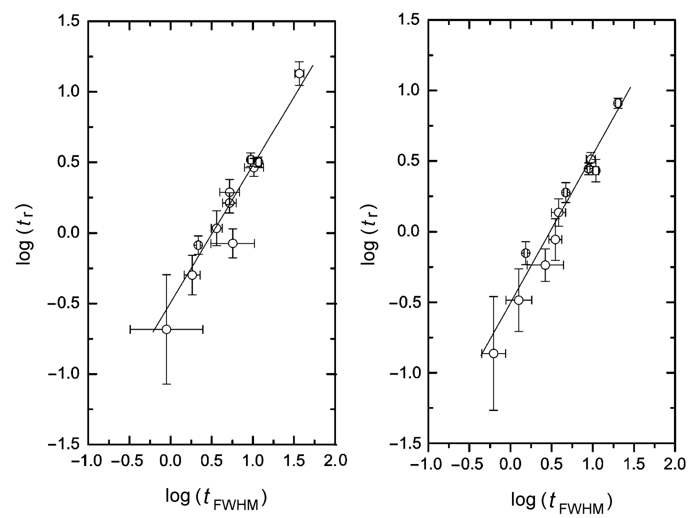

Fig. 4 Relationships between t_r and $t_{\rm FWHM}$ for the observed pulses based on sample 2. The left panel and the right panel present the pulses of the band B (7–40 keV) and C (30–400 keV), respectively. The two solid lines are the fit lines of their data.

The first two smaller standard deviations of the four intercepts in the two sample from the ones of the six dead lines obtained above theoretically are 0.043 for local Gaussian pulse and 0.120 for local exponential pulse, indicating that these four sequences are very close to the dead line of the local Gaussian pulse and that these observed pulses may have arisen from local Gaussian pulses. However, the conclusion is only preliminary which needs to be confirmed by larger samples in the future.

As shown in Figures 3 and 4, all the pulses, which are selected from long bursts, are longer than 0.5 s. Norris et al. (2001) pointed out that short bursts with $T_{90} < 2.6\,\mathrm{s}$ have different temporal behaviors from the long bursts. Do short and long pulses follow the same sequence in the t_r–$t_{\rm FWHM}$ plane and have the same temporal behavior? Motivated by this question, we select six short pulses from the 64 ms count data of 532 short GRBs (and call them sample 3) and 23 short pulses (shorter than 1 s) from long GRBs with the same criteria adopted in sample 2 (and call them sample 4). These short and long GRBs are detected by the BATSE instrument. We repeat the same calculation as above, and the results are plotted in the left panel of Figure 5.

We find from the left panel of Figure 5 that all the pulses (selected from short and long GRBs) follow the same sequence in the $t_r - t_{\rm FWHM}$ plane, with the shorter pulses at the end of this sequence, showing that short pulses (or bursts) have the same temporal behaviors as the long pulses, the only difference is that the quantity p (see Eqs. of (3) and (4)) is smaller for the short pulses.

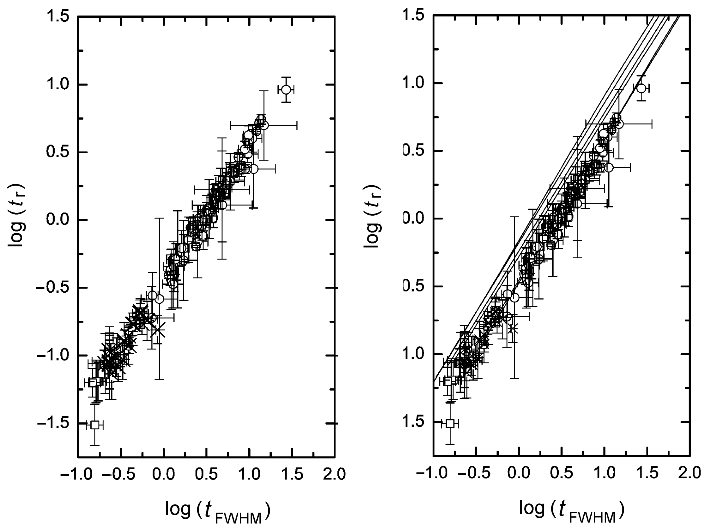

Fig. 5 Relationships between t_r and $t_{\rm FWHM}$ for the observed pulses. Left panel presents the observed pulses of the 3rd channel based on samples 1, 3 and 4. The open circle, open rectangle and cross present the pulses of sample 1, 3 and 4, respectively. Right panel is a combination of the left panel and the right panel in Fig. 2, where we take $R_{\rm c} = 3 \times 10^{15}$cm.

4 DISCUSSION AND CONCLUSIONS

All the analyses in this paper are based on Equation (1), which is for a fireball expanding isotropically with a constant Lorentz factor, $\Gamma > 1$. Equation (1) is suitable for describing the light curves of spherical fireballs or uniform jets. When considering a uniform jet and taking $\theta_{\max} = \Gamma^{-1}$ in Equation (1), we measure the τ_r and $\tau_{\rm FWHM}$ of the resulting light curves. They show no difference from those of spherical geometry, indicating that the relationships in the τ_r–$\tau_{\rm FWHM}$ plane are the same whether the gamma-ray burst pulses come from spherical fireballs or uniform jets.

It is an ubiquitous trend that the spectral indexes of many GRBs are observed to vary with time (see Preece et al. 2000). We wonder how the relationship would be if the rest frame spectrum evolves with time. As Preece et al. (2000) pointed out, the typical fitted value is $1.5 \sim -0.3$ for the low energy spectral index α, and is $-2 \sim -3$ for the high energy spectral index β. Therefore, sets of typical values of the indexes such as (–1.5, –2), (–0.3, –3) and (–0.8, –2.5) could be used to investigate the relationship. Calculations show that the two quantities, τ_r and $\tau_{\rm FWHM}$, are not significantly affected by the form of the rest frame radiation.

We find that, owing to the Doppler effect of the fireball surface (or the curvature effect), for any local pulse form, the width of the light curve would always be $t_{\rm FWHM} = k\Gamma^{-2}\Delta\tau_{\theta,{\rm FWHM}}\frac{R_{\rm c}}{c}$ (with different values of k for different local pulse forms, see Table 1). As derived in detail in Paper II, the width of the light curve of the local δ function pulse would be $\tau_{\rm FWHM} \simeq \frac{\sqrt{2}-1}{2}\Gamma^{-2}\Delta\tau$ (see eq.(48) in Paper II), where $\Delta\tau$ is the the observed time interval of the local δ function pulse, i.e., $\Delta\tau = 1 + \beta\tau_{\theta,0}$. Considering the correlation between τ and t, and taking $\tau_{\theta,0} = 0$, we obtain $t_{\rm FWHM} \simeq \frac{\sqrt{2}-1}{2}\Gamma^{-2}\frac{R_{\rm c}}{c} \simeq 2\,{\rm s}(\frac{R_{\rm c}}{10^{15}{\rm cm}})(\frac{\Gamma}{10^2})^{-2}$, which would be the lower limit of the width of the light curve for any local pulse form. Because of the relativistic beaming of the moving radiating particles, only the emission from a narrow cone with an opening angle of Γ^{-1} is observed. Ryde & Petrosian (2002) obtained that the curvature timescale resulting from relativistic effects is $\tau_{\rm ang} = 1.7\,{\rm s}\,(\frac{R_{\rm c}}{10^{15}{\rm cm}})(\frac{\Gamma}{10^2})^{-2}$ (see eq.(5) in their paper). Even as they pointed out, this is a lower bound for the observed duration of a pulse. Thus it can be seen that the curvature timescale and the lower limit of the width of light curves are comparable.

From Equations (3) and (6) we know that the only difference between the two panels, $t_r - t_{\rm FWHM}$ and $\tau_r - \tau_{\rm FWHM}$, is that different observed pulses, corresponding to the same Γ and $\Delta\tau_{\theta,{\rm FWHM}}$ but different values of $R_{\rm c}$, would correspond to one point in the $\tau_r - \tau_{\rm FWHM}$ plane while to different points in the $t_r - t_{\rm FWHM}$ plane, as they come from different values of $R_{\rm c}$, and these different points must be on a line with slope $B = 1.0$. However, the intercepts of the light curves in the two panels depend only on the form and width of the local pulses.

It is widely accepted in the scenario of standard fireball model that gamma-ray bursts arise from internal shocks at a distance of $R_{\rm c} \sim 10^{13} - 10^{17}$ cm (see Rees & Mészáros 1992, 1994; Mészáros & Rees 1993, 1994; Mészáros 1995; Katz 1994; Paczynski & Xu 1994; Sari & Piran 1997; Piran 1999; Spada et al. 2000; Ryde & Petrosian 2002; Piran 2005). To compare theoretical conclusions with the observed results in the $t_r - t_{\rm FWHM}$ plane, we merge the left panel of Figure 5 into the right panel of Figure 2 by applying Equations (5) and (6) and taking $R_{\rm c} = 3 \times 10^{15}$ cm. The results are plotted in the right panel of Figure 5, which are in good agreement with those predicted by Qin's model. We notice that the all observed pulses are below the dead line of local Gaussian form within their errors.

As shown above, for most of the observed pulses we have local pulse widths $\Delta\tau_{\theta,{\rm FWHM}} \geq 0.1$. Applying the relationship between τ_θ and t_θ, we obtain $\Delta t_{\theta,{\rm FWHM}} \geq 0.1\frac{R_{\rm c}}{c}$. As we take $\tau_{\theta,\min} = 0$ (i.e., $t_{\theta,\min} = t_{\rm c}$) in the above analysis, $R_{\rm c}$ is thus the radius of the fireball measured at $t_{\theta,\min}$. That is the time the pulse concerned begins to emit, which is generally assumed to be the stage that the fireball becomes optically thin and the photons created inside it can freely escape. Moreover, the fact that $\Delta\tau_{\theta,{\rm FWHM}} \geq 0.1$ indicates that the local pulse width is not more than one order of magnitude less than the time scale for the fireball to become optical thin for most of observed pulses. Its implication is not clear now because we do not know what results in the local pulses yet.

In fine, we come to the following conclusions: (1) the observed relationship between t_r and $t_{\rm FWHM}$ could be produced merely the curvature effect; (2) both long and short pulses follow the same sequence in the t_r–$t_{\rm FWHM}$ plane. If all observed pulses come from the same radius of the fireball (especially for the pulses in a burst), the shorter pulses have smaller value of p (here $p = \Gamma^{-2}\Delta\tau_{\theta,{\rm FWHM}}$), which might imply that short pulses come from narrower local pulses of larger Γ, and short bursts come from even narrowest local pulses of even largest Γ. This is a reasonable result if short GRBs are likely to be produced by the merger of compact objects while long GRBs result from the core collapse of massive stars; (3) all GRBs may arise intrinsically from local Gaussian pulses, which would have widths $\Delta\tau_{\theta,{\rm FWHM}}$ not less than 0.1, in agreement with the findings of Qin et al. (2005b); (4) the observed pulses that fall below the dead line of the local

Gaussian pulse would arise from the narrower local pulses (i.e., smaller than 1), and the shorter the pulse, the greater the deviation. However, we suspect that no observed pulses will fall far above the dead line of the local Gaussian pulse in the $t_r - t_{\rm FWHM}$ plane if they arise from a local Gaussian pulse in terms of the fireball model.

These features above may provide constraints on the intrinsic emission mechanism responsible for the GRBs.

Acknowledgements This work was supported by the Special Funds for Major State Basic Research Projects ("973") and the National Natural Science Foundation of China (NSFC, Nos. 10273019 and 10463001).

References

Band D., Matteson J., Ford L. et al., 1993, ApJ, 413, 281
Borgonovo L., Ryde F., 2001, ApJ, 548, 770
Cui X. H., Liang E. W., Lu R. J, 2005, Chin. J. Astron. Astrophys., 5, 151
Fenimore E. E., Madras C. D., Nayakshin, S., 1996, ApJ, 473, 998
Fishman G. J., Meegan C. A., Wilson R. B. et al., 1994, ApJS, 92, 229
Ford L. A., Band D. L., Mattesou J. L. et al., 1995, ApJ, 439, 307
Goodman J. 1986, ApJ, 308, L47
Ghirlanda G., Ghisellini G., Celotti A., 2004, A&A 422L, 55
Ghisellini G., Celotti A., Lazzati D., 2000, MNRAS, 313, L1
Jia L. W., Qin Y. P., ApJ, 631, L25
Katz J. I., 1994, ApJ, 422, 248
Kocevski D., Ryde F., Liang E., 2003, ApJ, 596, 389 (Paper I)
Lamb D. Q., Ricker G. R., Atteia J. L. et al. 2002, ApJ, submitted, astro-ph/0206151
Lee A., Bloom E. D., Petrosian V., 2000a, ApJS, 131, 1
Lee A., Bloom E. D., Petrosian V., 2000b, ApJS, 131, 21
Lu R. J., Qin Y. P., Zhang Z. B. et al., 2005a, MNRAS, in press, astro-ph/0509287
Lu R. J., Qin Y. P., 2005b, MNRAS, submitted, astro-ph/0508537
Mészáros P., Rees M. J., 1993, ApJ, 405, 278
Mészáros P., Rees M. J., 1994, MNRAS, 269, L41
Mészáros P., 1995, in Procs. 17th Texas Symp. Rel. Astroph., New York: NY Acad. Sci., 759, 440
Norris J. P., Nemiroff R. J., Bonnell J. T. et al., 1996, ApJ, 459, 393
Paczynski B., 1986, ApJ, 308, L43
Paczynski B., Xu G., 1994, ApJ, 427, 708
Piran T., 1999, Phys. Rep., 314, 575
Piran T., 2005, Reviews of Modern Physics, 76, 1143
Preece R. D., Pendleton G. N., Briggs M. S. et al., 1998, ApJ, 496, 849
Preece R. D., Briggs M. S., Mallozzi R. S. et al., 2000, ApJS, 126, 19
Qin Y. P., 2002, A&A, 396, 705
Qin Y. P., 2003, A&A, 407, 393
Qin Y. P., Zhang Z. B., Zhang F. W. et al., 2004, ApJ, 617, 439 (Paper II)
Qin Y. P., Dong Y. M., Lu R. J. et al., 2005a, ApJ, 632, 1008
Qin Y. P., Lu R. J., 2005b, MNRAS, 362, 1085
Ramirez-Ruiz E., Fenimore E. E., 2000, ApJ, 539, 712
Rees M. J., Mészáros P., 1992, MNRAS, 258, 41
Rees M. J., Mészáros P., 1994, ApJ, 430, L93
Ryde F., Svensson R., 2000, ApJ, 529, L13
Ryde F., Petrosian V., 2002, ApJ, 578, 290
Ryde F., Borgonovo L., Larsson S. et al., 2003, A&A, 411, L331
Schaefer B. E., Teegaeden B. J., Fantasia S. F. et al., 1994, ApJS, 92, 285
Schmidt M., 2001, APJ, 559, L79
Sari R., Piran T., 1997, MNRAS, 287, 110
Spada M., Panaitescu A., Mészáros P., 2000, ApJ, 537, 824
Zhang B., Mészáros P., 2004, IJMPA, 19, 2385